Higgs production in e and real gamma collisions

Ken Sasaki (Yokohama National U.)

In collaboration with

H. Watanabe

Y. Kurihara (KEK)

T. Uematsu (Kyoto U.)

Physics Letters B (2013) arXiv:1311.1601[hep-ph]
Physical Review D90 (2014) arXiv:1403.4703[hep-ph]

May 22, 2017, Photon 2017, CERN

Outline

1. Introduction and motivations
2. Higgs production in e and real γ collision in SM
3. Two-photon and Z-photon fusion diagrams
4. W-related and Z-related diagrams
5. Differential cross section
6. Numerical analysis
7. $e^-\gamma$ collisions in e^-e^- collider
8. Summary

1. Introduction and motivations

- A Higgs particle was found at the LHC

  Is it the SM Higgs boson , a SUSY Higgs boson,

  a Higgs boson of a different model?

- Future e^+e^- colliders: CLIC, ILC
  FCC-ee, CEPC
  ……

- Before e+ beams are ready,

  other options are possible:

  - an e^-e^- option
  - an $e^-\gamma$ option

    use one e- beam to produce high energy photons

I.Gizburg, G.Kotkin, V.Serbo, V.Telnov
A.De Roeck: hep-ph/0311138v1(2003)
V.Telnov: Photon2015

1. Introduction and motivations

$e^-\gamma$ collider based on e^-e^- beams

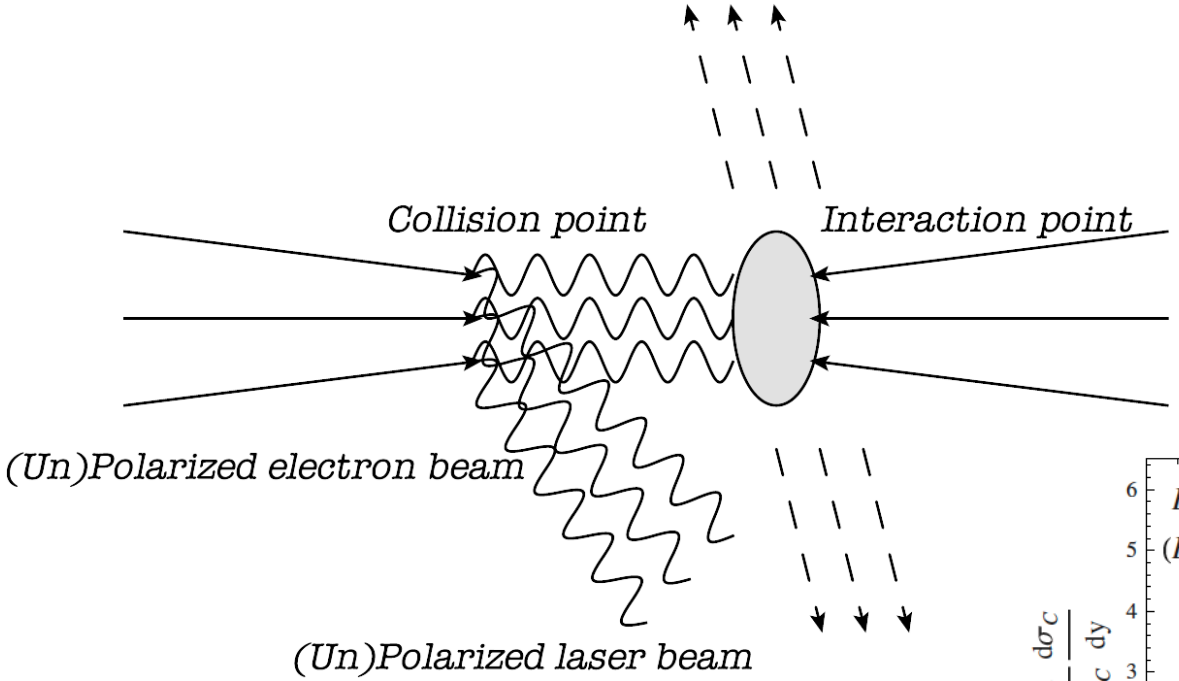

Compton backward scattering

$$e^-\gamma_{\text{Laser}} \rightarrow e^-\gamma$$

can transfer 80% of e^- energy to γ

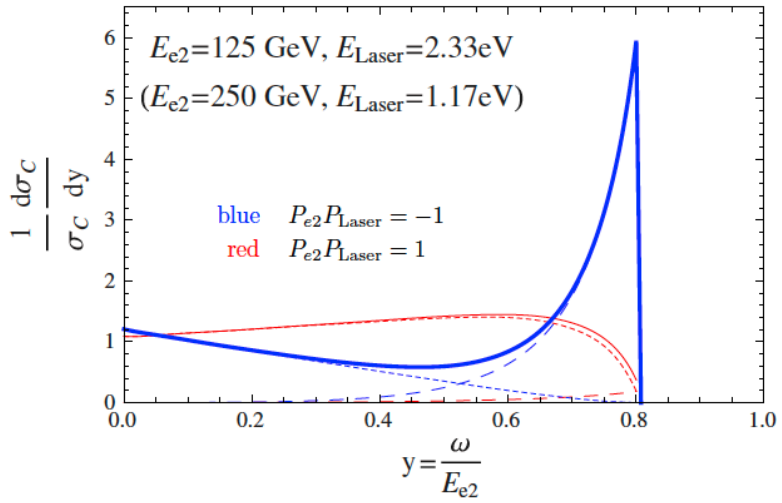

1. Introduction and motivations

- In two-photon fusion process for Higgs production in $e\gamma$ collision, we may observe the transition form factor of Higgs

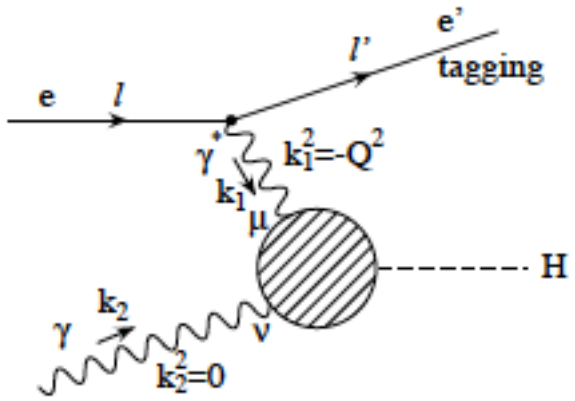

in analogy of the $\gamma^*\gamma \to \pi^0$ transition form factor observed at BaBar and Belle

2 Higgs production in e- and real γ collision in SM

- Higgs are produced by loop diagrams

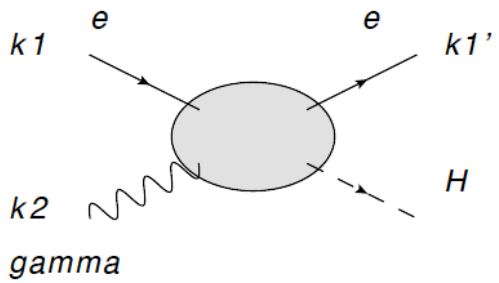

At one-loop level

$\gamma\gamma$-fusion diagrams
$\mathbf{Z}\gamma$-fusion diagrams
W-related diagrams
Z-related diagrams

$$k_1^2 = k_1'^2 = m_e^2 = 0\,; \quad p_h^2 = m_h^2,$$

$$\begin{aligned} s &= (k_1 + k_2)^2 = 2k_1 \cdot k_2\,, \quad t = (k_1 - k_1')^2 = -2k_1 \cdot k_1' = q^2, \\ u &= (k_1 - p_h)^2 = (k_1' - k_2)^2 = -2k_1' \cdot k_2 = m_h^2 - s - t \\ k_2^2 &= 0\,, \qquad k_2^\beta\, \epsilon(k_2)_\beta = 0 \end{aligned}$$

2 Higgs production in e- and real γ collision in SM

- Calculation is done in unitary gauge
- Use of FeynCalc, PaVeReduce[Oneloop[p,-----]]
- Amplitudes are expressed in analytical form

using the results of

Denner, Nierste, Scharf (1991)
Keith Ellis, Zanderighi (2008)
Denner, Dittmaier (2010)

3. Two-photon and Z-photon fusion diagrams

$e \cdot e \cdot \gamma$ coupling : $i(-e)\gamma_\mu$

$t \cdot t \cdot \gamma$ coupling : $i(q_t e)\gamma_\mu$

$e \cdot e \cdot Z$ coupling : $i\frac{g}{4\cos\theta_W}\gamma_\mu(f_{Ze} + \gamma_5)$ with $f_{Ze} = -1 + 4\sin^2\theta_W$

$t \cdot t \cdot Z$ coupling : $i\frac{g}{4\cos\theta_W}\gamma_\mu\,[f_{Zt} - \gamma_5]$ with $f_{Zt} = 1 - \frac{8}{3}\sin^2\theta_W$

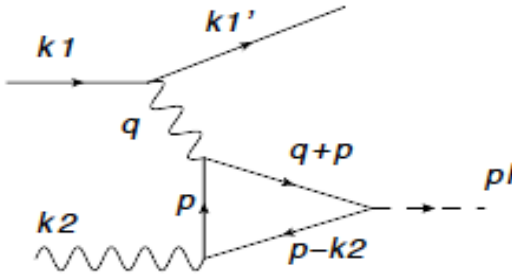

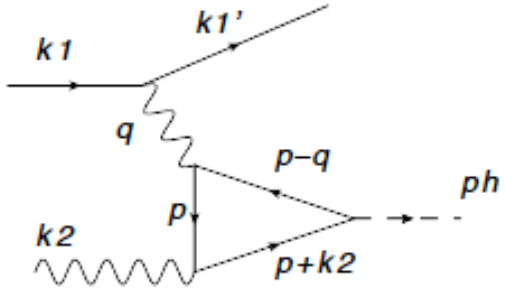

Higgs $\cdot\, t \cdot t$ coupling : $-i\frac{gm_t}{2m_W}$

Higgs $\cdot\, W \cdot W$ coupling : $igm_W g_{\mu\nu}$

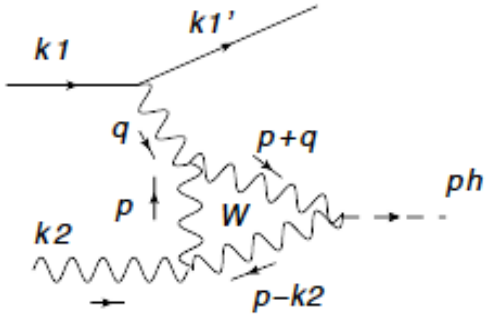

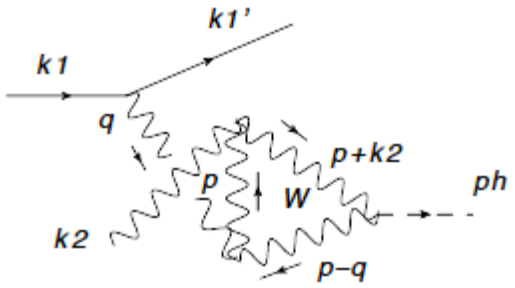

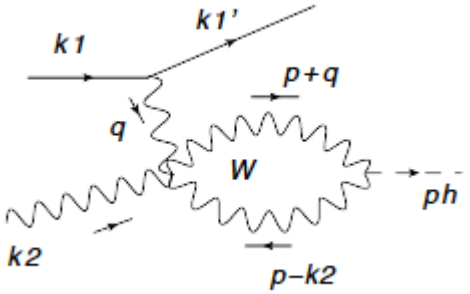

$Z_\mu(k_1)$-$W^+_\nu(k_2)$-$W^-_\lambda(k_3)$ coupling: $-ig\cos\theta_W\left[(k_1-k_2)_\lambda g_{\mu\nu} + (k_2-k_3)_\mu g_{\nu\lambda} + (k_3-k_1)_\nu g_{\lambda\mu}\right]$

A_μ-Z_ν-W^+_α-W^-_β coupling: $-ieg\cos\theta_W\left[2g_{\mu\nu}g_{\alpha\beta} - g_{\mu\alpha}g_{\nu\beta} - g_{\mu\beta}g_{\nu\alpha}\right]$

3. Two-photon and Z-photon fusion diagrams

- Contribution of two-photon fusion diagrams

$$A_{\gamma\gamma} = \left(\frac{e^3 g}{16\pi^2}\right)\left[\overline{u}(k_1')\gamma_\mu u(k_1)\right]\frac{1}{t}\left(g^{\mu\beta} - \frac{2k_2^\mu q^\beta}{m_h^2 - t}\right)\epsilon_\beta(k_2)\; F_{\gamma\gamma}$$

$$F_{\gamma\gamma} = \frac{2m_t^2}{m_W} N_c Q_t^2 \; S_{(T)}^{\gamma\gamma}(t, m_t^2, m_h^2) - m_W S_{(W)}^{\gamma\gamma}(t, m_W^2, m_h^2)$$

  - Top quark loops:

$$S_{(T)}^{\gamma\gamma}(t, m_t^2, m_h^2) = 2 - \frac{2t}{m_h^2 - t} B_0(t; m_t^2, m_t^2) + \frac{2t}{m_h^2 - t} B_0(m_h^2; m_t^2, m_t^2)$$
$$+\left\{4m_t^2 - m_h^2 + t\right\} C_0(m_h^2, 0, t; m_t^2, m_t^2, m_t^2)$$

$$B_0(p^2; m_1^2, m_2^2) \equiv \frac{(2\pi\mu)^{4-n}}{i\pi^2}\int \frac{d^n k}{\left[k^2 - m_1^2\right]\left[(k+p)^2 - m_2^2\right]}$$

$$C_0(p_1^2, p_2^2, p_3^2; m_1^2, m_2^2, m_3^2) \equiv \frac{(2\pi\mu)^{4-n}}{i\pi^2}\int \frac{d^n k}{\left[k^2 - m_1^2\right]\left[(k+p_1)^2 - m_2^2\right]\left[(k+p_1+p_2)^2 - m_3^2\right]}$$

  - W boson loops:

$$S_{(W)}^{\gamma\gamma}(t, m_W^2, m_h^2) = 6 + \frac{m_h^2 - t}{m_W^2} - \frac{m_h^2 t}{2m_W^4}$$
$$+\frac{t\left(12m_W^4 + 2m_W^2\left(m_h^2 - t\right) - m_h^2 t\right)}{2m_W^4\left(m_h^2 - t\right)}\left[B_0(m_h^2; m_W^2, m_W^2) - B_0(t; m_W^2, m_W^2)\right]$$
$$+\left\{\frac{t\left(m_h^2 - 2t\right)}{m_W^2} + 12m_W^2 - 6m_h^2 + 6t\right\} C_0(m_h^2, 0, t; m_W^2, m_W^2, m_W^2)$$

3. Two-photon and Z-photon fusion diagrams

- Contribution of Z-photon fusion diagrams

$$A_{Z\gamma} = \left(\frac{eg^3}{16\pi^2}\right)\left[\overline{u}(k_1')\gamma_\mu\left(f_{Ze}+\gamma_5\right)u(k_1)\right]\frac{1}{t-m_Z^2}\left(g^{\mu\beta}-\frac{2k_2^\mu q^\beta}{m_h^2-t}\right)\epsilon_\beta(k_2)\ F_{Z\gamma}$$

$$F_{Z\gamma} = -\frac{m_t^2}{8m_W\cos^2\theta_W}N_cQ_tf_{Zt}S_{(T)}^{Z\gamma}(t,m_t^2,m_h^2)+\frac{m_W}{4}S_{(W)}^{Z\gamma}(t,m_W^2,m_h^2)$$

  - Top quark loops: $S_{(T)}^{Z\gamma}(t,m_t^2,m_h^2)=S_{(T)}^{\gamma\gamma}(t,m_t^2,m_h^2)$
  - W boson loops: $S_{(W)}^{Z\gamma}(t,m_W^2,m_h^2)=S_{(W)}^{\gamma\gamma}(t,m_W^2,m_h^2)$

The contribution of two-photon and Z-photon fusion diagrams have the same transition form factors

4. W-related and Z-related diagrams

- Other contributions to Higgs production in e - γ collision

$e \cdot \nu \cdot W$ coupling : $i\frac{g}{2\sqrt{2}}\gamma_\mu(1-\gamma_5)$

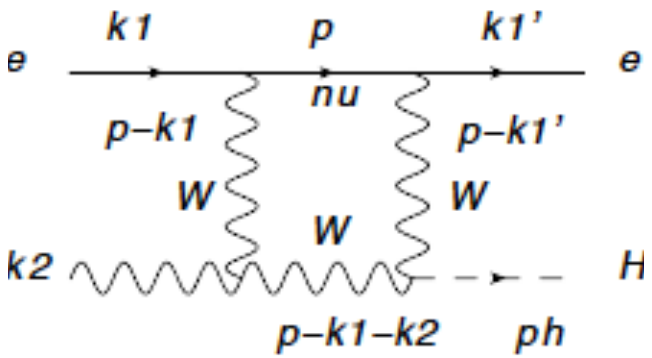

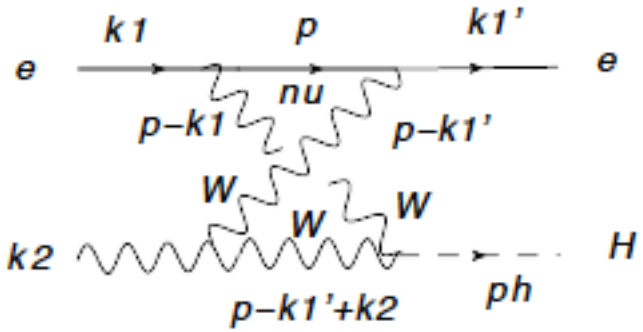

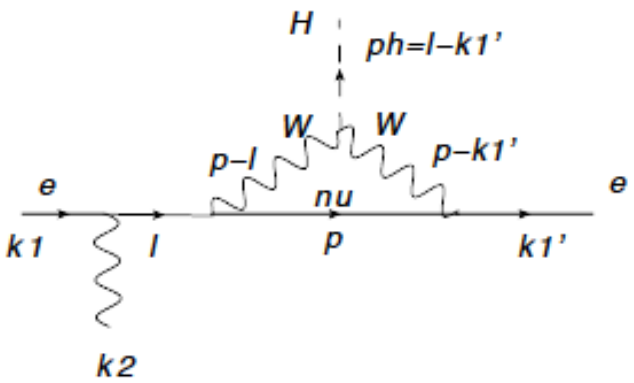

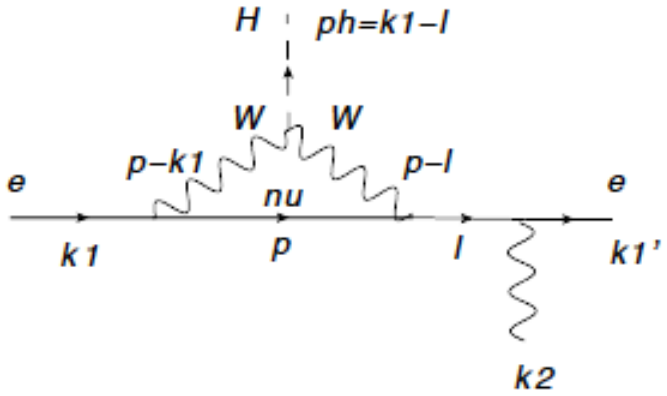

4. W-related and Z-related diagrams

$e \cdot e \cdot Z$ coupling : $i\frac{g}{4\cos\theta_W}\gamma_\mu(f_{Ze}+\gamma_5)$ with $f_{Ze} = -1 + 4\sin^2\theta_W$

Higgs $\cdot Z \cdot Z$ coupling : $i\frac{gm_Z}{\cos\theta_W}g_{\mu\nu}$

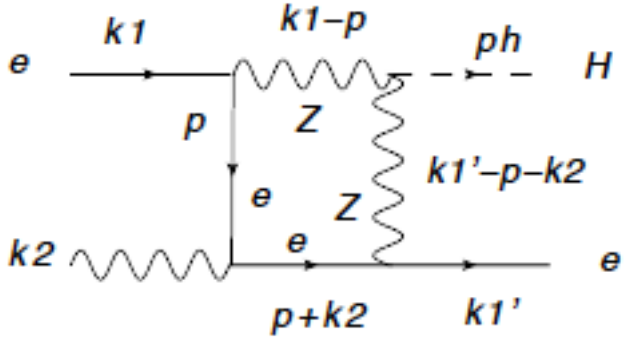

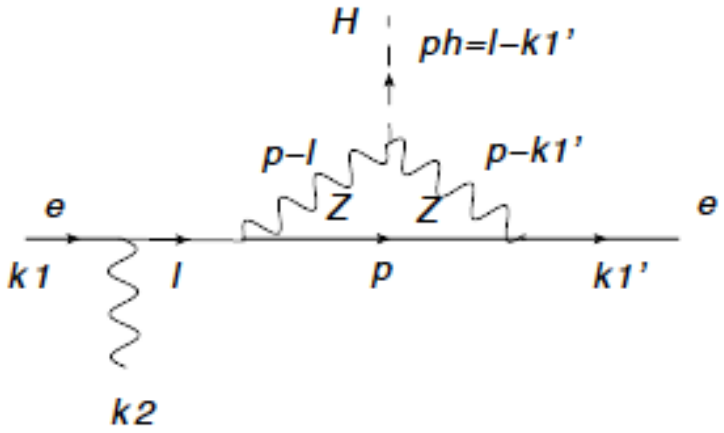

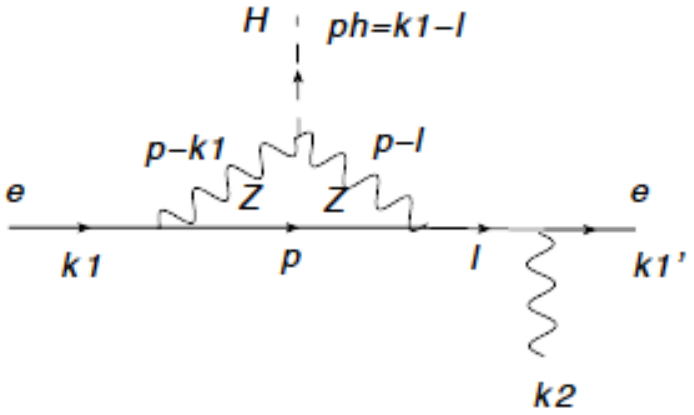

4. W-related and Z-related diagrams

- Contribution of W-related diagrams

$$A_{W\nu_e} = \left(\frac{eg^3}{16\pi^2}\right)\frac{m_W}{4}\left[\overline{u}(k_1')\, F_{(W\nu_e)\beta}\, (1-\gamma_5)u(k_1)\right]\epsilon(k_2)^\beta$$

$$F_{(W\nu_e)\beta} = \left(\frac{2k_{1\beta}\not{k}_2}{s} - \gamma_\beta\right)S^{W\nu_e}_{(k_1)}(s,t,m_h^2,m_W^2) + \left(\frac{2k_{1\beta}'\not{k}_2}{u} + \gamma_\beta\right)S^{W\nu_e}_{(k_1')}(s,t,m_h^2,m_W^2)$$

where

Note: $S^{W\nu_e}_{(k_1')} \to 0 \quad \text{as} \quad u \to 0$

$S^{W\nu_e}_{(k_1)}(s,t,m_h^2,m_W^2)$ and $S^{W\nu_e}_{(k_1')}(s,t,m_h^2,m_W^2)$

: expressed as a linear combination of

$$B_0(s;0,m_W^2) \quad B_0(u;0,m_W^2) \quad B_0\left(t;m_W^2,m_W^2\right) \quad B_0\left(m_h^2;m_W^2,m_W^2\right)$$

$$C_0\left(0,0,s;m_W^2,m_W^2,0\right) \quad C_0\left(0,0,u;m_W^2,m_W^2,0\right) \quad C_0\left(0,0,t;m_W^2,0,m_W^2\right)$$

$$C_0\left(0,s,m_h^2;m_W^2,0,m_W^2\right) \quad C_0\left(0,u,m_h^2;m_W^2,0,m_W^2\right) \quad C_0\left(0,t,m_h^2;m_W^2,m_W^2,m_W^2\right)$$

$$D_0\left(0,0,0,m_h^2;s,t;m_W^2,m_W^2,0,m_W^2\right) \quad D_0\left(0,0,0,m_h^2;t,u;m_W^2,0,m_W^2,m_W^2\right)$$

- When the initial electron is right-handed, $A_{W\nu_e} = 0$

4. W-related and Z-related diagrams

- Contribution of Z-related diagrams

$$A_{Ze} = \left(\frac{eg^3}{16\pi^2}\right)\left(-\frac{m_Z}{16\cos^3\theta_W}\right) \times \left[\overline{u}(k_1')\, F_{(Ze)\beta}\, (f_{Ze} + \gamma_5)^2 u(k_1)\right] \epsilon(k_2)^\beta$$

$$F_{(Ze)\beta} = \left(\frac{2k_{1\beta}\not{k}_2}{s} - \gamma_\beta\right) S^{Ze}_{(k_1)}(s,t,m_h^2,m_Z^2) + \left(\frac{2k'_{1\beta}\not{k}_2}{u} + \gamma_\beta\right) S^{Ze}_{(k_1')}(s,t,m_h^2,m_Z^2)$$

where

Note: $S^{Ze}_{(k_1')} \to 0 \quad \text{as} \quad u \to 0$

$S^{Ze}_{(k_1)}(s,t,m_h^2,m_Z^2)$ and $S^{Ze}_{(k_1')}(s,t,m_h^2,m_Z^2)$

: expressed as a linear combination of

$B_0(s;0,m_Z^2)$ $B_0(u;0,m_Z^2)$ $B_0\left(m_h^2;m_Z^2,m_Z^2\right)$

$C_0\left(0,0,s;m_Z^2,0,0\right)$ $C_0\left(0,0,u;m_Z^2,0,0\right)$ $C_0\left(0,s,m_h^2;m_Z^2,0,m_Z^2\right)$ $C_0\left(0,u,m_h^2;m_Z^2,0,m_Z^2\right)$

$D_0\left(0,0,0,m_h^2;s,u;m_Z^2,0,0,m_Z^2\right)$

- Collinear divergences appear in $C_0\left(0,0,s;m_Z^2,0,0\right)$ $C_0\left(0,0,u;m_Z^2,0,0\right)$ $D_0\left(0,0,0,m_h^2;s,u;m_Z^2,0,0,m_Z^2\right)$ but they are cancel out when they are added

5. Differential cross section

- Linear Collider : good polarizations for the initial colliding beams

  Initial electron helicity: $P_e = \pm 1$

  Initial photon helicity: $P_\gamma = \pm 1$

- Differential cross section

$$\frac{d\sigma_{(e\gamma\to eH)}(P_e,P_\gamma)}{dt} = \frac{1}{16\pi s^2} \times \left\{ \sum_{\text{final electron spin}} |A(P_e,P_\gamma)|^2 \right\}$$

$$A(P_e,P_\gamma) = A_{\gamma\gamma}(P_e,P_\gamma) + A_{Z\gamma}(P_e,P_\gamma) + A_{W\nu_e}(P_e,P_\gamma) + A_{Ze}(P_e,P_\gamma)$$

- Angular momentum conservation in forward and backward directions
  - In the massless limit of electron, its helicity is conserved

$A(P_e,P_\gamma)$ vanishes at $\theta = 0$ $\qquad A(P_e,P_\gamma) \propto t$

$A(P_e,P_\gamma)$ with $P_eP_\gamma = -1$ vanishes at $\theta = \pi$ $\qquad A(P_eP_\gamma = -1) \to 0$ as $u \to 0$

5. Differential cross section

- To obtain $A(P_e, P_\gamma)$:

$$u(k_1) \to \frac{1+P_e\gamma_5}{2}\, u(k_1)$$

$$\epsilon(k_2,\pm 1)^*_\alpha \epsilon(k_2,\pm 1)_\beta = -\frac{1}{2}\, g_{\alpha\beta} \pm \frac{i}{2}\left(g_{\alpha 1} g_{\beta 2} - g_{\alpha 2} g_{\beta 1}\right)$$

In the frame where the initial photon is moving in the z-direction

- Contributions from $\gamma\gamma$ fusion, $Z\gamma$ fusion, "W-ν_e" and "Z-e" diagrams

$$\frac{d\sigma_{(\gamma\gamma)}(P_e,P_\gamma)}{dt} = \frac{1}{16\pi\ s^2} \times \left\{ \sum_{\text{final electron spin}} |A_{\gamma\gamma}(P_e,P_\gamma)|^2 \right\}$$

$$= \frac{1}{16\pi\ s^2}\left(\frac{e^3 g}{16\pi^2}\right)^2 \left(-\frac{1}{t}\right) {F_{\gamma\gamma}}^2 \left\{ \frac{s^2+u^2}{(s+u)^2} + P_\gamma P_e \left(1 - \frac{2u}{s+u}\right)\right\},$$

5. Differential cross section

$$\frac{d\sigma_{(Z\gamma)}(P_e,P_\gamma)}{dt} = \frac{1}{16\pi\ s^2}\left(\frac{eg^3}{16\pi^2}\right)^2 \frac{-t}{(t-m_Z^2)^2}\ {F_{Z\gamma}}^2$$
$$\times\left\{(f_{Ze}^2+2P_e f_{Ze}+1)\frac{s^2+u^2}{(s+u)^2}+P_\gamma(P_e f_{Ze}^2+2f_{Ze}+P_e)\left(1-\frac{2u}{s+u}\right)\right\},$$

$$\frac{d\sigma_{(W\nu_e)}(P_e,P_\gamma)}{dt} = \frac{1}{16\pi s^2}\left(\frac{eg^3}{16\pi^2}\right)^2 \frac{m_W^2}{8}(-t)(1-P_e)\left\{\left[\left|S_{(k_1)}^{W\nu_e}(s,t,m_h^2,m_W^2)\right|^2+\left|S_{(k_1')}^{W\nu_e}(s,t,m_h^2,m_W^2)\right|^2\right]\right.$$
$$\left.+P_\gamma\left[-\left|S_{(k_1)}^{W\nu_e}(s,t,m_h^2,m_W^2)\right|^2+\left|S_{(k_1')}^{W\nu_e}(s,t,m_h^2,m_W^2)\right|^2\right]\right\},$$

$$\frac{d\sigma_{(Ze)}(P_e,P_\gamma)}{dt} = \frac{1}{16\pi s^2}\left(\frac{eg^3}{16\pi^2}\right)^2\left(\frac{m_Z}{16\cos^3\theta_W}\right)^2(-t)$$
$$\times\left\{(f_{Ze}^4+4P_e f_{Ze}^3+6f_{Ze}^2+4P_e f_{Ze}+1)\left[\left|S_{(k_1)}^{Ze}(s,t,m_h^2,m_Z^2)\right|^2+\left|S_{(k_1')}^{Ze}(s,t,m_h^2,m_Z^2)\right|^2\right]\right.$$
$$+P_\gamma(P_e f_{Ze}^4+4f_{Ze}^3+6P_e f_{Ze}^2+4f_{Ze}+P_e)\left[\left|S_{(k_1)}^{Ze}(s,t,m_h^2,m_Z^2)\right|^2\right.$$
$$\left.\left.-\left|S_{(k_1')}^{Ze}(s,t,m_h^2,m_Z^2)\right|^2\right]\right\}.$$

We see $\dfrac{d\sigma_{(W\nu_e)}(P_e=+1)}{dt}=0$ $\dfrac{d\sigma(P_eP_\gamma=-1)}{dt}\to 0 \quad \text{as} \quad u\to 0$

6. Numerical analysis

- Parameters

$$m_h = 125\ \text{GeV}\ , \quad m_t = 173\ \text{GeV}\ , \quad m_Z = 91\ \text{GeV}\ , \quad m_W = 80\ \text{GeV}$$
$$\cos\theta_W = \frac{m_W}{m_Z}\ , \qquad e^2 = 4\pi\alpha_{em} = \frac{4\pi}{128}\ , \qquad g = \frac{e}{\sin\theta_W}\ .$$

- t-dependence $\sqrt{s} = 200\ \text{GeV}$

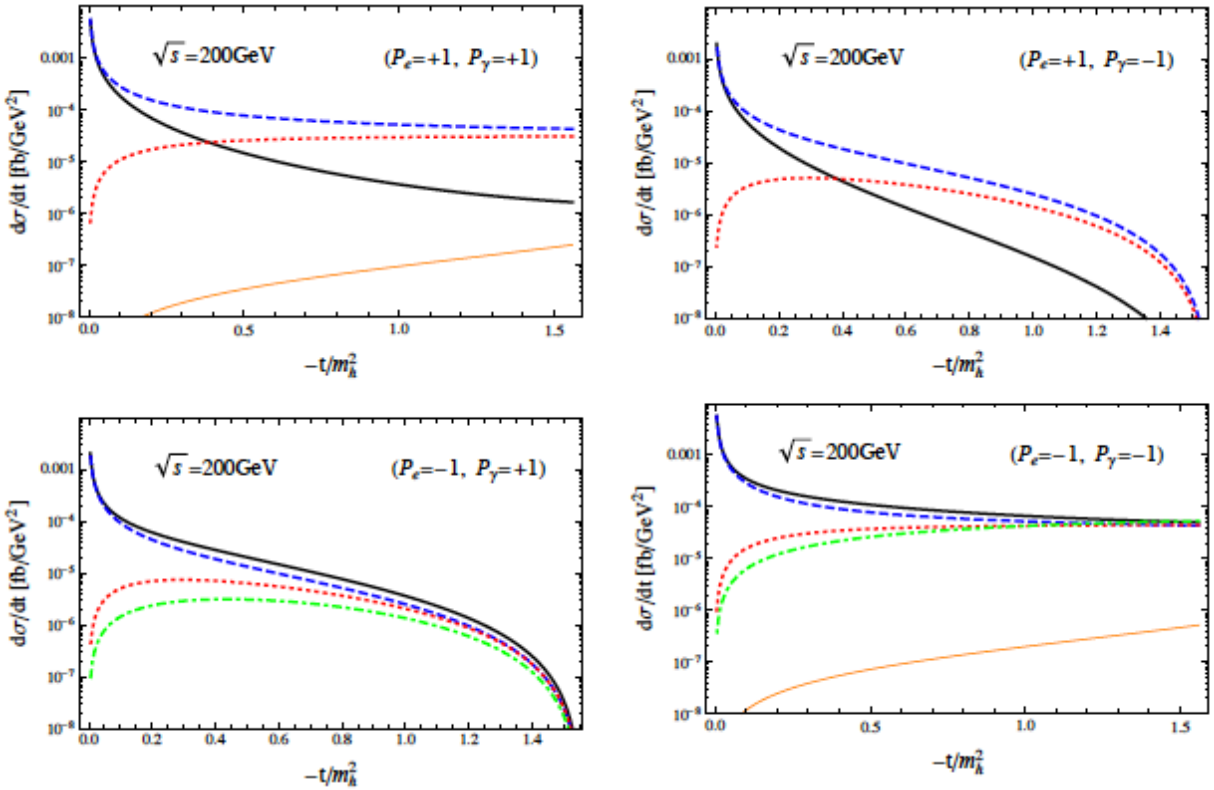

Black	Full
Blue	$\gamma\gamma$
Red	$\mathbf{Z}\gamma$
Green	W-related
Orange	Z-related

6. Numerical analysis

- t-dependence $\sqrt{s} = 400\ \mathrm{GeV}$

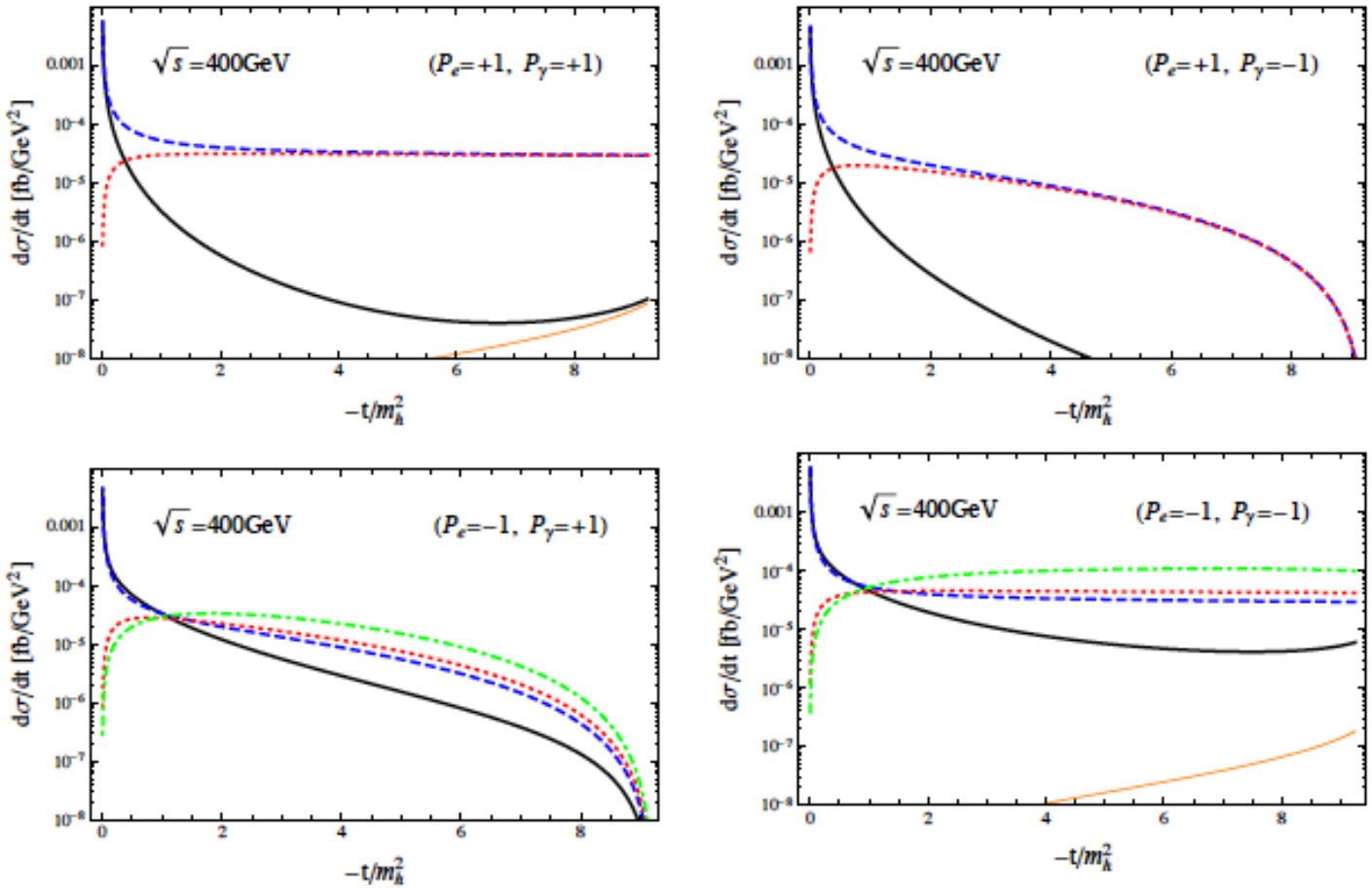

Black	Full
Blue	$\gamma\gamma$
Red	$\mathbf{Z}\gamma$
Green	W-related
Orange	Z-related

- The contribution from "Z-e" diagrams is negligibly small

6. Numerical analysis

- t-dependence
  - The case $P_e = -1$

    for $-t/m_h^2 \leq 1$, a dominant contribution comes from the $\gamma\gamma$ fusion diagrams

    for $1 < -t/m_h^2 < 1.5$, the contributions from the $\gamma\gamma$ fusion, $Z\gamma$ fusion and "W-ν_e" diagrams becomes the same order

    for $-t/m_h^2 > 1.5$, the contribution from "W-ν_e" diagrams prevails other two

    The interference between $A_{\gamma\gamma}$ and $A_{Z\gamma}$ works constructively

    $A_{\gamma\gamma}$ and $A_{W\nu_e}$ works destructively

  - The case $P_e = +1$

    No contribution from "W-ν_e" diagrams

    The interference between $A_{\gamma\gamma}$ and $A_{Z\gamma}$ works destructively

    Its effect is large even at small $-t/m_h^2$

    $d\sigma_{(e\gamma\to eH)}/dt$ decreases rather rapidly as $-t/m_h^2$ increases

6. Numerical analysis

- s-dependence

$$\sigma_{(e\gamma\to eH)}(s, P_e, P_\gamma) = \int_{\text{cut}} dt \frac{d\sigma_{(e\gamma\to eH)}(s, P_e, P_\gamma)}{dt}$$

$$10^\circ \le \theta \le 170^\circ$$

Black	Full
Blue	$\gamma\gamma$
Red	$\mathbf{Z}\gamma$
Green	W-related
Orange	Z-related

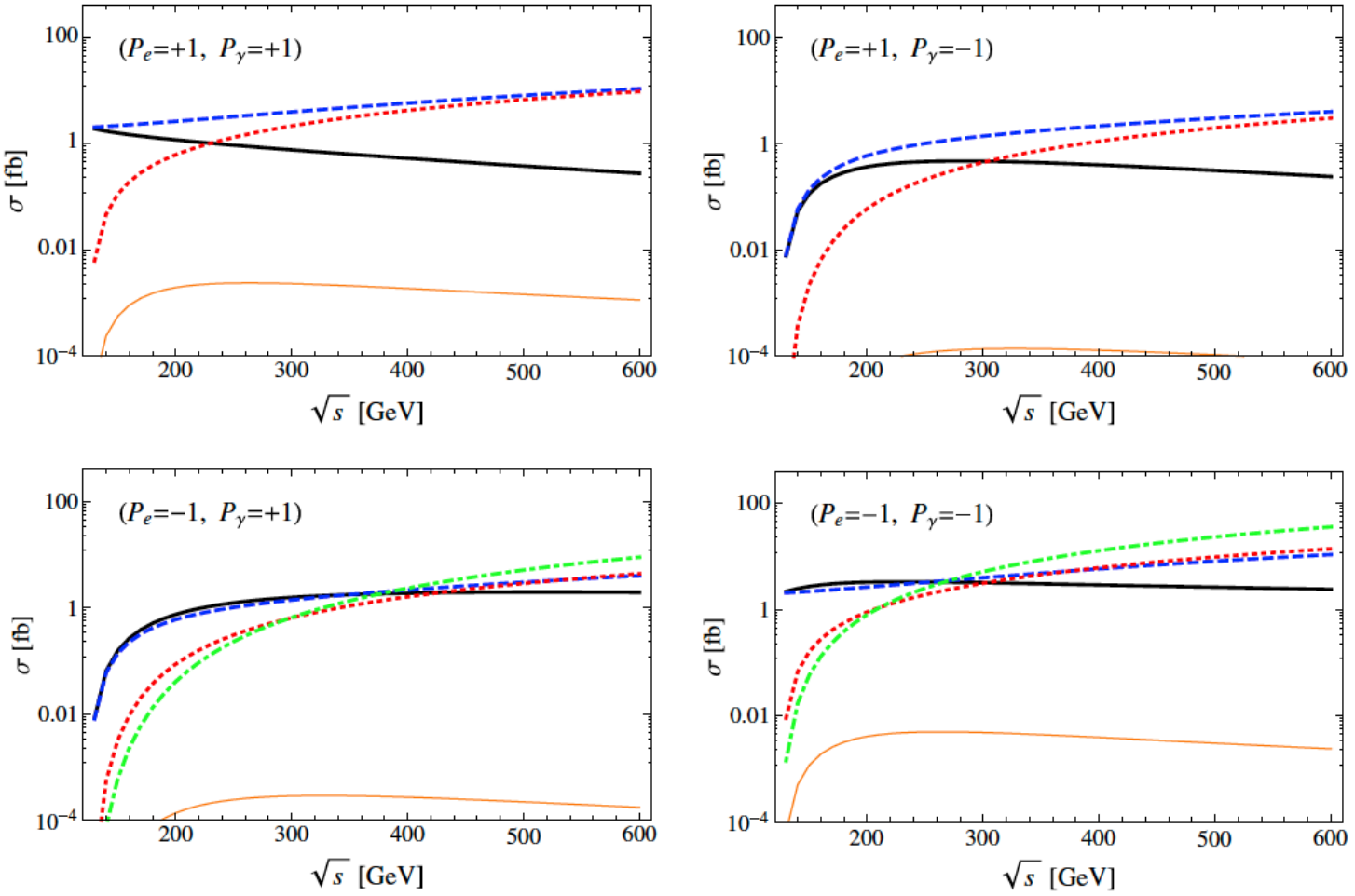

6. Numerical analysis

- s-dependence

  Higgs production cross section $\sigma_{(e\gamma\to eH)}$

  - The case $P_e P_\gamma = -1$
    - is very small at $\sqrt{s} = 130\ \mathrm{GeV}$
    - Increases rapidly to a few femtobarn at around $\sqrt{s} = 200\ \mathrm{GeV}$
    - stays about the same from $\sqrt{s} > 200\ \mathrm{GeV}$

  - The case $P_e P_\gamma = +1$
    - $\sigma_{(e\gamma\to eH)}$ is large even at small $\sqrt{s}$
    - remains roughly flat at a few femtobarn

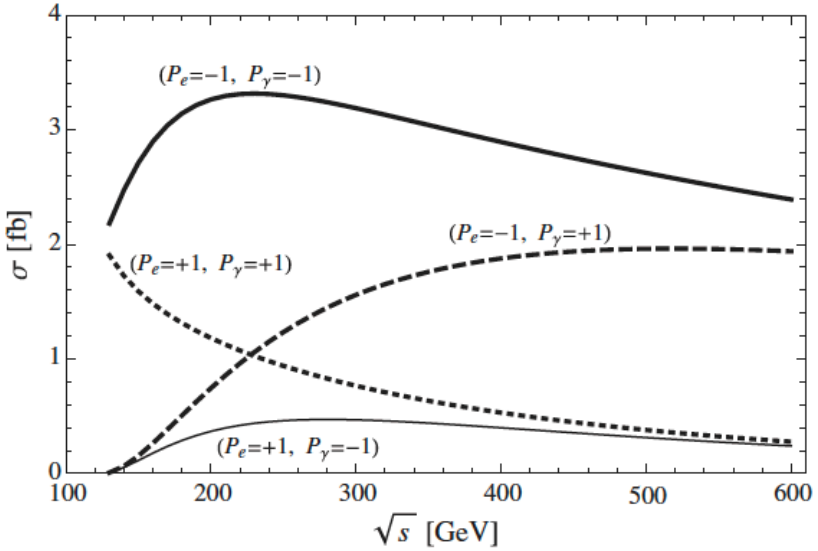

7. $e^-\gamma$ collisions in e^-e^- collider

A high-intensity photon beam is produced by laser light backward scattering off a high-energy electron beam

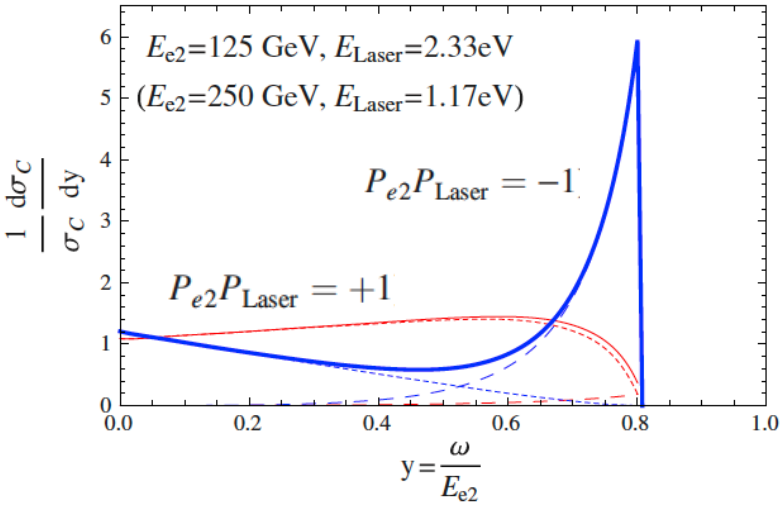

Analysis of the cross section of Higgs boson production through the $b\bar{b}$ decay channel in $e^-\gamma$ collisions in e^-e^- collider

$$\sigma_{e\gamma\text{collision}}(s_{ee}, E_{\text{Laser}}, P_{e1}, P_{e2}, P_{\text{Laser}}) = \sum_{P_\gamma} \int dy N(y, E_{e2}, E_{\text{Laser}}, P_{e2}, P_{\text{Laser}}, P_\gamma)\sigma_{(e\gamma\to eH)}(s, P_{e1}, P_\gamma)$$

The $b\bar{b}$ channel in $e^-\gamma$ collisions has a substantial background

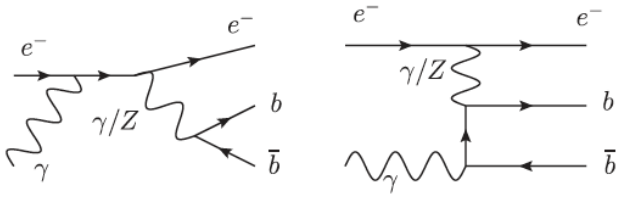

FIG. 10. Examples of background processes for $e+\gamma \to e+b+\bar{b}$.

A huge background appears at the Z-boson pole

7. $e^-\gamma$ collisions in e^-e^- collider

Monte Carlo result

TABLE I. Higgs boson production cross section and significance in an $e^-\gamma$ collision in an e^-e^- collider for the cases (i) $E_{\text{Laser}} = 2.33$ eV, $E_{e2} = 125$ GeV, $\sqrt{s_{ee}} = 250$ GeV and (ii) $E_{\text{Laser}} = 1.17$ eV, $E_{e2} = 250$ GeV, $\sqrt{s_{ee}} = 500$ GeV, and for each combination of polarizations P_{e1} and P_{Laser}. P_{e2} is chosen to be $-P_{\text{Laser}}$.

$\sqrt{s_{ee}}$ GeV	P_{e1}	P_{Laser}	σ_{cut} fb	$S/\sqrt{B}$
250	1	−1	0.50	6.17
	1	1	0.36	4.48
	−1	−1	0.80	4.51
	−1	1	1.53	8.68
500	1	−1	0.11	2.93
	1	1	0.19	1.31
	−1	−1	1.22	10.6
	−1	1	1.01	6.8

The significance is calculated by taking samples in the region

$$120\text{GeV} \leq m_{b\bar{b}} \leq 130\text{GeV}$$

at the parton level

The angle cuts

$$10^\circ \leq \theta_{e^-} \leq 170^\circ$$

$$10^\circ \leq \theta_{b(\bar{b})} \leq 170^\circ$$

8. Summary

- Higgs boson production in $\mathbf{e^-\gamma}$ collision was investigated in SM.
- The EW one-loop contributions to the amplitude for $e+\gamma \Longrightarrow e+H$ were obtained in analytical form.
- We find:
  - Both the differential cross section $d\sigma_{(e\gamma\to eH)}(s,P_e,P_\gamma)/dt$ and the cross section $\sigma_{(e\gamma\to eH)}(s,P_e,P_\gamma)$ are significantly dependent on the polarizations of the electron and photon beams
  - The interferences between $\gamma\gamma$ and $\mathbf{Z}\gamma$ -fusion diagrams and between $\gamma\gamma$ and W-related diagrams are important factors affecting the behaviors of both the differential cross section and cross section.
  - Contribution of Z-related diagrams is extremely small and can be neglected
- The cross section of the Higgs boson production through the $b\bar{b}$ decay channel in $\mathbf{e^-\gamma}$ collision in $\mathrm{e^-e^-}$ collider was analyzed.
  - We obtained large values of the significance $\sqrt{S/B}$ for the Higgs boson production for both $\sqrt{s_{ee}}=250\ \mathrm{GeV}$ and $\sqrt{s_{ee}}=500\ \mathrm{GeV}$
- Therefore we conclude that the Higgs boson will be clearly observed in $\mathbf{e^-\gamma}$ collision experiments

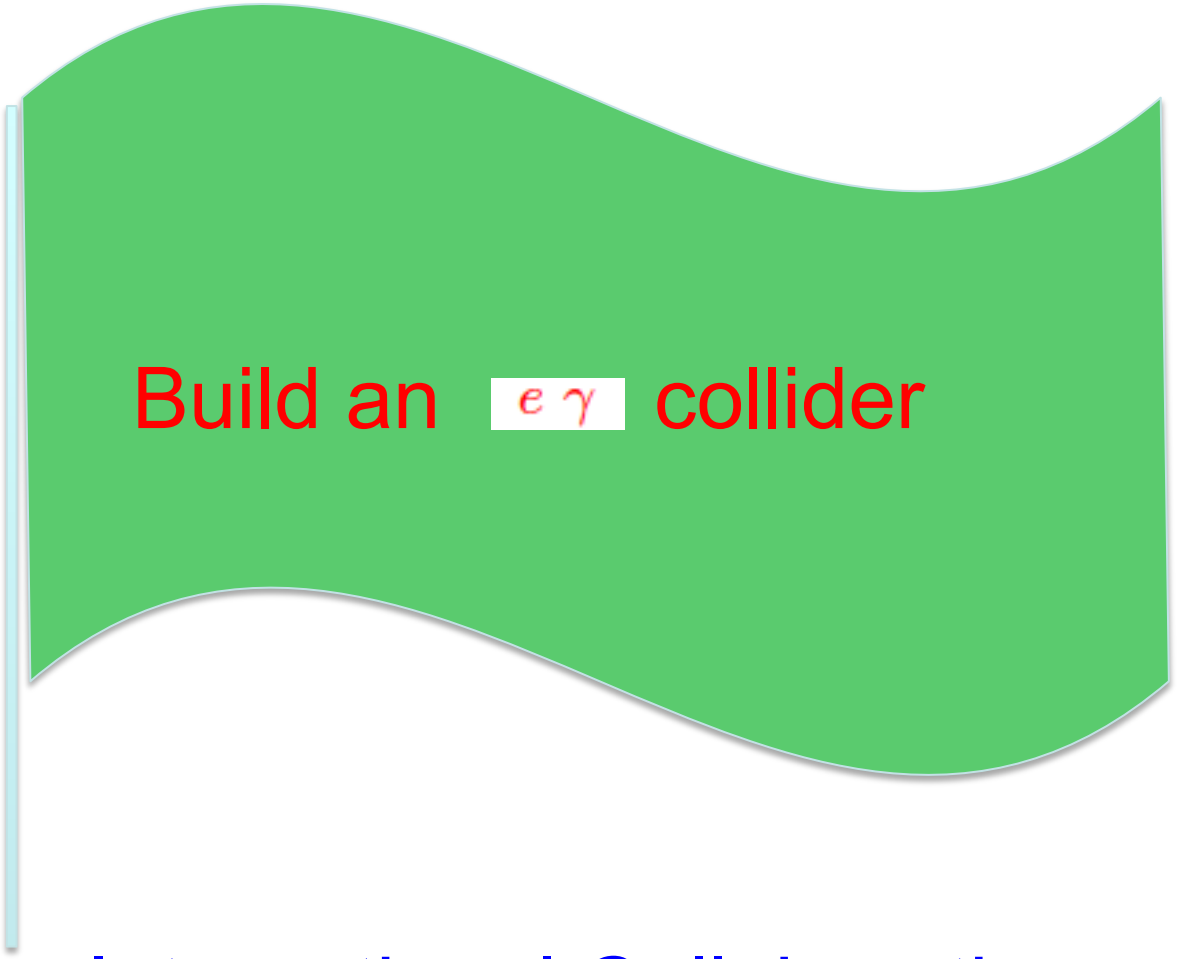

International Collaboration

Backup Slides

Collinear Singularities

$$C_0(0,0,s;m_Z^2,0,0) = -\left(\frac{4\pi\mu^2}{m_Z^2}\right)^\epsilon \frac{1}{s}\Big\{ \frac{1}{\epsilon}\Big[\log(s_Z-1)-i\pi\Big] - \frac{1}{2}\Big[\log(s_Z-1)-i\pi\Big]^2 - \mathrm{Li}_2\left(\frac{s_Z-1}{s_Z}\right) - \frac{1}{2}\log^2\left(\frac{s_Z}{s_Z-1}\right) + \frac{\pi^2}{3} - i\pi\log\left(\frac{s_Z}{s_Z-1}\right)\Big\}$$

$$C_0(0,0,u;m_Z^2,0,0) = -\left(\frac{4\pi\mu^2}{m_Z^2}\right)^\epsilon \frac{1}{u}\Big\{ \frac{1}{\epsilon}\log(1-u_Z) + \mathrm{Li}_2\left(\frac{-u_Z}{1-u_Z}\right) - \frac{1}{2}\log^2(1-u_Z)\Big\}$$

$$s_Z = \frac{s}{m_Z^2}, \quad u_Z = \frac{u}{m_Z^2}, \quad h_Z = \frac{m_h^2}{m_Z^2}$$

$$x_{Z_+} = \frac{1}{2}\Big(1+i\sqrt{\frac{4}{h_Z}-1}\Big)$$

$$x_{Z_-} \equiv \frac{1}{2}\Big(1-i\sqrt{\frac{4}{h_Z}-1}\Big)$$

$$\begin{aligned} D_0(0,0,0,m_h^2;s,u;m_Z^2,0,0,m_Z^2) &= D_0(0,0,m_h^2,0;s,u;0,0,m_Z^2,m_Z^2) \\ &= \frac{1}{su-m_Z^2(s+u)}\Big\{\Big(\frac{4\pi\mu^2}{m_Z^2}\Big)^\epsilon e^{-\epsilon\gamma_E}\times\frac{1}{\epsilon}\Big[-\Big[\log(s_Z-1)-i\pi\Big]-\log(1-u_Z)\Big] \\ &+2\mathrm{Li}_2\left(\frac{s_Z-1}{s_Z}\right)-2\mathrm{Li}_2\left(-\frac{u_Z}{1-u_Z}\right)-2\mathrm{Li}_2\left(\frac{1}{(1-s_Z)(1-u_Z)}\right) \\ &+\mathrm{Li}_2\left(-\frac{x_{Z_+}}{x_{Z_-}(1-s_Z)}\right)+\mathrm{Li}_2\left(-\frac{x_{Z_-}}{x_{Z_+}(1-s_Z)}\right)+\mathrm{Li}_2\left(1+\frac{x_{Z_+}(1-u_Z)}{x_{Z_-}}\right)+\mathrm{Li}_2\left(1+\frac{x_{Z_-}(1-u_Z)}{x_{Z_+}}\right) \\ &+\log^2\left(\frac{s_Z}{s_Z-1}\right)+2\log\Big((s_Z-1)(1-u_Z)\Big)\log\left(\frac{s_Z+u_Z-u_Zs_Z}{(s_Z-1)(1-u_Z)}\right)+2\log(s_Z-1)\log(1-u_Z) \\ &+\log^2(1-u_Z)+\log\left(1+\frac{x_{Z_+}}{x_{Z_-}(1-s_Z)}\right)\left\{\log\left(-\frac{x_{Z_+}}{x_{Z_-}}\right)-\log(s_Z-1)\right\} \\ &+\log\left(1+\frac{x_{Z_-}}{x_{Z_+}(1-s_Z)}\right)\left\{\log\left(-\frac{x_{Z_-}}{x_{Z_+}}\right)-\log(s_Z-1)\right\} \\ &+i\pi\left[2\log\left(\frac{s_Z}{s_Z+u_Z-u_Zs_Z}\right)+\log\left(1+\frac{x_{Z_+}}{x_{Z_-}(1-s_Z)}\right)+\log\left(1+\frac{x_{Z_-}}{x_{Z_+}(1-s_Z)}\right)\right] \\ &-\frac{2\pi^2}{3}\Big\} \end{aligned} \qquad \text{(B3}$$

- They appear in combination of $\Big\{sC_0\left(0,0,s;m_Z^2,0,0\right)+uC_0\left(0,0,u;m_Z^2,0,0\right) +[m_Z^2(s+u)-su]D_0\left(0,0,0,m_h^2;s,u;m_Z^2,0,0,m_Z^2\right)\Big\}$